frontiers in Earth Science

ORIGINAL RESEARCH
published: 11 August 2021
doi: 10.3389/feart.2021.734458

Nature of Volatile Organic Matter in Lake Sediments as a Reflection of Paleoclimate Changes Occurring at 4 ka in the Central Qaidam Basin

Xiaohang Lu[1,2,3], *Yongsheng Zhang*[4], *Lei Yi*[1,2], *Zhe Ma*[1,2,3]*, *Weigang Su*[1,2,3], *Xiaobao Liu*[1,2,3] *and Fengqing Han*[1,2]*

[1]Key Laboratory of Comprehensive and Highly Efficient Utilization of Salt Lake Resources, Qinghai Institute of Salt Lakes, Chinese Academy of Sciences, Xining, China, [2]Qinghai Provincial Key Laboratory of Geology and Environment of Salt Lakes, Xining, China, [3]Qinghai Institute of Salt Lakes, University of Chinese Academy of Sciences, Beijing, China, [4]The Third Geological Exploration Institute of Qinghai Province, Xining, China

OPEN ACCESS

Edited by:
Zhang Chengjun,
Lanzhou University, China

Reviewed by:
Weiguo Liu,
Institute of Earth Environment (CAS), China
Mingrui Qiang,
South China Normal University, China

***Correspondence:**
Zhe Ma
mazhe.isl@foxmail.com
Fengqing Han
hanfq@isl.ac.cn

Specialty section:
This article was submitted to Quaternary Science, Geomorphology and Paleoenvironment, a section of the journal Frontiers in Earth Science

Received: 01 July 2021
Accepted: 02 August 2021
Published: 11 August 2021

Citation:
Lu X, Zhang Y, Yi L, Ma Z, Su W, Liu X and Han F (2021) Nature of Volatile Organic Matter in Lake Sediments as a Reflection of Paleoclimate Changes Occurring at 4 ka in the Central Qaidam Basin. Front. Earth Sci. 9:734458. doi: 10.3389/feart.2021.734458

This study explores the paleoclimate changes around the 4 ka BP period in the central Qaidam Basin (QB), assessing the differences in spectral characteristics and organic composition of salt lake sediments under different climate change conditions. Sediment samples (10-m-depth profile) were collected from the middle of dry salt flats in East Taijinar Lake (China). Sediment organic matter (SOM) was assessed by Fourier transform infrared spectroscopy (FTIR) and gas chromatography-mass spectrometry (GC-MS). Results showed a significant difference in the TOC content of sediments with different lithological characteristics. A lower TOC content in salt-bearing strata was attributed to the extreme sedimentary environment with minimal exogenous inputs. FTIR spectroscopy revealed that the SOM in sediments included aliphatic C, ketones and alcohols. Sediments of salt-bearing strata generally exhibited a rise in the content of ketone C=O groups and a decrease in aliphatic C, with an equal content of alcohols compared with silty sand. Therefore, exogenous OM and the content of TOC in silty sand strata are higher than in salt-bearing strata, indicating that the paleoclimate became warmer and wetter after 4 ka BP. GC-MS analysis showed a significant difference between the phenol and aldehyde content in different strata, further indicating that the paleoclimate changed from dry to relatively warm around 4 ka BP. Seven organic compound types were identified in SOM, including aldehydes, hydrocarbons, phenols, esters, ketones, alcohols, and furans. Different strata exhibited different distributions of organic compounds, with particularly high concentrations of aldehydes in salt-bearing strata and phenols in silty sand. Correlation analysis was performed between detrital minerals and OM types in all samples. Results showed a strong positive correlation between detrital minerals and phenols and a strong negative correlation between detrital minerals and aldehydes, with a negative correlation also identified between detrital minerals and ketones. Overall, the reduction in volatile organic compounds demonstrates that the paleoclimate changed from cooler and dry to wet and warm around the 4 ka BP period in the central QB, with the carbon preference index and *n*-alkane values further demonstrating these results. This

study also confirms the importance of volatile organic compound monitoring to assess paleoclimate changes.

Keywords: sediment organic matter, FTIR, GC-MS, detrital minerals, correlation analysis, *n*-alkane, paleoclimate

INTRODUCTION

The Qaidam Basin, located at the northern margin of the Tibetan Plateau (TP), is one of the highest and most arid regions worldwide (Yu and Lai, 2012). The QB is influenced by three major climatic systems, including the East Asian summer monsoon (EASM), the westerlies and the Indian monsoon (IM). Reconstructions of the paleoclimate in the QB have attracted much research attention due to its sensitive to climatic variability (Xiang et al., 2013; Stauch et al., 2017). Different geological archives, including ice cores (Thompson et al., 1997), eolian sand and loess sections (Sun et al., 2007; Stauch, 2015), and lake sediments (Lu et al., 2011; Ma et al., 2019) have been used to reconstruct climate changes in the TP at different locations. In particular, the organic matter (OM) present in salt lake sediments, such as *n*-alkanes, fatty acids and lignin, can serve as a highly sensitive indicator for environmental reconstructions.

Salt lakes are saline environments containing relatively high salt concentrations, which widely occur worldwide (Zheng, 2011). Owing to the complexity and specific geotectonic-climatic conditions required for salt lake formation, the sedimentary characteristics of saline lakes differ from other lake environments. Saline lake sediments are a product of the physical-geographical and geological environment, with the development of sedimentary strata retaining information on the changing surrounding environment. Therefore, saline lake sediments provide a sensitive record of paleoclimatic and paleoenvironmental changes (Zheng et al., 2016). The OM accumulated in saline lake sediments is considered to reflect changes in terrestrial vegetation, as well as the hydrological conditions and aquatic plant productivity in lakes, providing a historical source of information on the regional environment (Prokopenko et al., 1999; Meyers and Teranes, 2001; Lücke and Brauer, 2004; Wischnewski et al., 2011; Aichner et al., 2012).

The sources of sediment organic matter (SOM) in salt lake sediments are complex and can include planktonic and benthic fauna and flora, in addition to terrestrial material from riverine and anthropogenic inputs. SOM can exist in anaerobic environments for a long period of time, being subjected to a variety of geological processes. The partition or distribution of OM in sediments mainly depends on the functional groups and molecular structures contained in OM and the surface properties of sediment mineral particles (Kleber et al., 2007; Liang et al., 2011). It has been reported that salinity may be an important factor in determining the distribution of OM (Means, 1995; Tremblay et al., 2005), with the sources and redox conditions of OM in sediments also known to affect its distribution behavior (Wilson and Xenopoulos, 2009; Riedel et al., 2013). For example, the high concentration of organic carbon and the C/N ratio in the surface sediments of Bled lake (Slovenia) has been shown to depend on the sediment oxidation environment (Muri and Wakeham, 2006). Therefore, the chemical and functional properties of OM in sediments depend on its source material and biogeochemical history (Tfaily et al., 2017). The assessment of OM in sediments allows a better understanding of the biogeochemical cycling of carbon in lake and sediment environments (Tuo et al., 2011; Fan et al., 2017). However, few studies have explored the distribution behavior of OM in salt lake sediments.

In the early stages of the diagenetic process, there is a close relationship between SOM and mineral particles (Keil et al., 1994). For example, early authigenic quartz fills primary pores and decreases interparticle porosity, controlling the distribution of migrated OM during early diagenesis, subsequently affecting the development and volume of OM pores in siliceous shale gas windows (Zhao et al., 2017a). Biomineralized calcite plays an important role in the function of many organisms and in turn, uses organic macromolecules to control crystal growth (Hakim et al., 2017). Furthermore, the surface properties of minerals may affect important interaction processes, such as organic matter interactions (Valdrè et al., 2012). In the later stages of sediment diagenesis, mineral grains provide a degree of protection and reduce the rate of OM decomposition in sediments (Wang and Lee, 1993). Despite the low level of OM reserves in sediments, the structure and strength of OM adsorption on mineral surfaces is relevant to various environmental applications, such as CO_2 storage and contamination remediation (Quicksall et al., 2008; Brown and Calas, 2012).

However, conflicting results have been obtained using different lake sediment proxies for moisture reconstruction, such as in Lake Qinghai (China) (Chen et al., 2016 and references therein). An et al. (2012) proposed that the northeastern Tibetan Plateau climate was wet during the early Holocene period, based on carbonate analysis. However, it has also been proposed that the early Holocene climate was relatively dry, based on analysis of pollen assemblages (Shen et al., 2005). In addition, previous studies on climate change in the QB have reported varying results for the late Holocene period around 4 ka BP. Sun et al. (2019) and Wu et al. (2018) proposed that a rapid cold and drought event occurred around 4 ka BP, leading to the gradual drought in the QB in the late Holocene period. Xiang et al. (2013) suggested that the climate was mainly warm and dry after 3830 BP, with a warm cool and extremely dry climate predicted during 3,040–2,600 ka BP based on both *n*-alkane and pollen proxies. In contrast, Chen et al. (2008) proposed that the topography of the TP and the adjacent Asian highlands led to a dry climate in the early Holocene period, while the climate became relatively humid (less dry) after 8 ka BP. It is of note, most studies have mainly been focused on the eastern or southern regions of the TP which are sensitive and ideally located to reflect the paleoclimate change of the whole TP region (An et al., 2012;

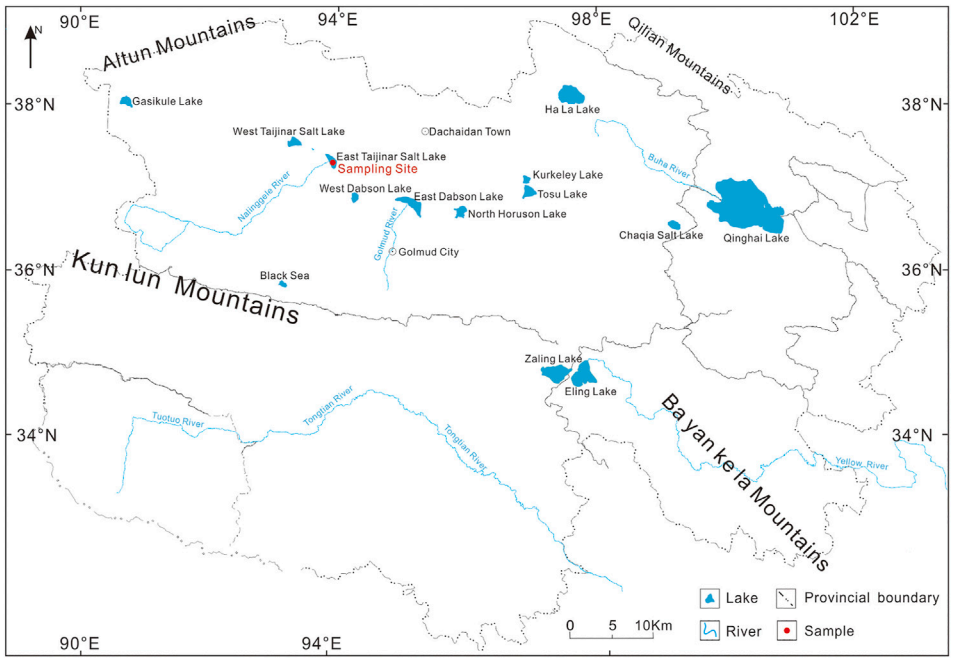

FIGURE 1 | Map of the sampling site and lakes in the Qinghai Province (China).

Cheng et al., 2013), while little research has been performed on the central QB region. Therefore, it is important to clarify the interpretations of environmental data in the central QB region around 4 ka BP. Also, few studies have assessed the chemical composition of SOM in these regions, especially in salt lake sediments. Due to the high salinity of salt lakes and the presence of various toxic ions (Co, Ni, and Mn), the composition of SOM in salt lake sediments is relatively unique (Liu et al., 2018; Isaji et al., 2019), making a precise understanding of SOM composition in salt lake sediments valuable information. In this study, samples were collected directly in the central QB region for analysis of the OM composition and distribution characteristics, to reflect the palaeoclimate changes at 4 ka BP. Meanwhile, some established palaeoclimate indicators, such as detrital mineral flux, nC_{31}/nC_{29} ratio, and CPI, were used to verify the results.

The aim of this study was to assess climate changes in the late Holocene period at 4 ka BP, in the middle of the QB using OM in lake sediments. First, Fourier transform infrared (FTIR) spectroscopy and gas chromatography-mass spectrometry (GC-MS) were used to investigate the composition of OM in salt lake sediments. FTIR spectroscopy provides insight into the chemical functions of OM based on its functional groups (Derenne and Quénéa, 2015), while GC-MS is an established analytical method for volatile organic compounds (Ene et al., 2012), providing a molecular fingerprint for OM based on its molecular weight and elemental composition (Stashenko and Martínez, 2014). Then, the paleoenvironmental changes in the middle of QB around the 4 ka BP period were reconstructed based on the *n*-alkane distribution and comparison with the OM in salt lake sediments.

MATERIALS AND METHODS

Geological Background

The East Taijinar salt lake (37°21′54″–37°36′05″N, 93°45′33″–94°06′48″W) is located in the Tertiary anticline structural depression belt of the QB (Qinghai, China) (**Figure 1**). The formation of this salt lake is associated with the uplift of the Qinghai-Tibet Plateau, the strong tectonic movement of the QB, and the migration of residual salt-forming brine from western to central and eastern regions (Zhang et al., 1987). The lake is mainly supplied by the Nalinggele River from the Kunlun Mountains in the southwest. The brine subtype is magnesium sulfate with a pH of 7.9 (Zheng and Liu, 2009). The East Taijinar salt lake spans approximately 300 km^2, which includes a lake area of 100 and 200 km^2 of dry salt flats. The dominant sediment component in the upper stratum of the salt lake area is halite, along with small amounts of mirabilite and gypsum and other relatively simple minerals such as quartz and feldspar.

Sample Collection

Sediment samples were collected from a depth profile (13.5 m) in the middle of the dry salt flats using a polyvinyl chloride corer (30 mm inner diameter and 250 mm length). All samples were collected in clean vertical sections. They were covered with a black cloth and sealed in black plastic bags, then wrapped with tape to avoid exposure to light or contamination.

The lithological profile of the core samples from top to bottom was as follows: silty sand strata (SS) from 0 to 8.0 m,

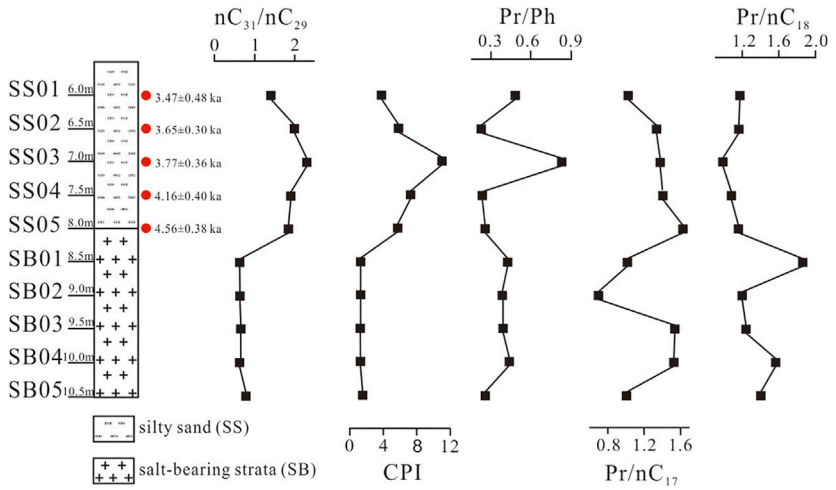

FIGURE 2 | OSL sample site, chronology, CPI, Pr/Ph, Pr/nC_{17}, and Pr/nC_{18} values of the 10 samples from different strata of the East Taijinar salt lake sediments.

TABLE 1 | Results of the OSL dating of SS sediments (Ma et al., 2021).

Sample	Depth (m)	Grain size (μm)	K (%)	Th (ppm)	U (ppm)	Water content (%)	Dose rate (Gy/ka)	*De* (Gy)	OSL age (ka)
SS01	6.0	4–11	3.16 ± 0.04	14.76 ± 0.70	3.31 ± 0.40	17 ± 5	4.71 ± 0.33	16.37 ± 1.92	3.47 ± 0.48
SS02	6.5	38–63	2.63 ± 0.04	12.58 ± 0.70	2.94 ± 0.40	15 ± 5	3.92 ± 0.29	14.32 ± 0.50	3.65 ± 0.30
SS03	7.0	4–11	2.92 ± 0.04	12.65 ± 0.70	4.21 ± 0.40	9 ± 5	5.11 ± 0.37	19.23 ± 1.21	3.77 ± 0.36
SS04	7.5	4–11	2.83 ± 0.04	12.60 ± 0.70	5.18 ± 0.40	19 ± 5	4.61 ± 0.34	19.18 ± 1.21	4.16 ± 0.40
SS05	8.0	38–63	1.92 ± 0.04	9.19 ± 0.70	2.171 ± 0.40	14 ± 5	2.93 ± 0.23	13.35 ± 0.41	4.56 ± 0.38

Note: SS, silty sand.

consisted of loose silty sand; salt-bearing strata (SB) from 8.0 to 13.5 m, harder and denser than that of silty sand, composed mainly of white halite. The first sample was collected at a depth of 0.5 m, with subsequent samples collected from below this along a vertical depth profile at intervals of 0.5 m, resulting in 27 samples being collected for each profile. In this study, a total of ten samples were selected for analysis, including five from each of the two different lithologic strata zones, with the depth and age details for each sample shown in **Figure 2**.

All selected sediment samples were dated using optically stimulated luminescence in the Luminescence Dating Laboratory of the Qinghai Institute of Salt Lakes, Chinese Academy of Sciences. The dating of all samples have been done in our previous work, and the reliability and accuracy of the dating results have been discussed in the paper (Ma et al., 2021). The effective age of the salt-bearing strata could not be identified because of the low content of quartz and feldspar, although according to the lithology, this layer should be the product of an arid environment in the 4 ka BP period. The result of the OSL dating with their equivalent dose (*De*) values are given in **Table 1**. The remaining samples were stored in sterile polyethylene bags and maintained at 4°C. Prior to analysis, samples were freeze-dried, ground, and then passed through a 200-μm mesh sieve.

FTIR Analysis

FTIR spectroscopy was performed at room temperature, using the KBr pellet technique. The samples were dried immediately prior to analysis to minimize interference due to moisture. OM characterization by infrared spectroscopy involved the collection of FTIR absorbance spectra in the mid-infrared region from 4,000 to 400 cm^{-1}. Confirmation of the chemical bonds and functional groups attributed to absorption peaks in the FTIR spectra was performed using previously reported literature.

GC-MS Analysis

The OM content in all ten samples from 0 to 8.0 m and 8.5–13 m depths were analyzed using gas chromatography mass spectrometry (GC-MS), using a Thermo TRACE 1300 Series Gas Chromatograph combined with a TSQ 8000 Evo MS detector (Thermo Scientific, United States). Solid-phase microextraction (SPME) was performed using a 50/30 μm divinylbenzene/carboxen/polydimethylsiloxane (DVB/CAR/PDMS) fiber (Supelco, Bellefonte, PA, United States). GC analysis was carried out using a 30 cm × 0.25 mm DB-Wax column (0.25 μm film thickness; J&W Scientific Inc., United States). Prior to GC-MS analysis, the 2 g of samples were heated at 60°C for 60 min in an incubating box, then subjected to SPME for 30 min at a constant temperature of 60°C, with the injection volume set to 1 μl and an injector temperature of 250°C. The GC oven was maintained

TABLE 2 | Mineral composition and TOC content in sediment samples with different lithological caharcteristics.

No.	Halite	Quartz	Sodium feldspar	Muscovite	Gypsum	Chlorite	Calcite	Dolomite	TOC
					%				
SS01	7	30	18	19	13	6	5	2	0.14
SS02	16	32	12	21	6	7	4	2	0.12
SS03	7	30	15	27	6	8	5	2	0.17
SS04	4	41	19	18	3	6	6	3	0.12
SS05	5	36	18	19	7	7	5	3	0.15
SB01	96	2	nd	nd	1	nd	1	nd	0.04
SB02	91	1	nd	nd	8	nd	nd	nd	0.03
SB03	93	2	nd	nd	5	nd	nd	nd	0.02
SB04	95	2	nd	nd	2	nd	1	nd	0.04
SB05	62	3	nd	nd	35	nd	nd	nd	0.03

Note: SS, silty sand; SB, salt-bearing strata; nd, not detected.

at 50°C for 2 min and then increased to 220°C at 3°C/min and maintained for 1 min. Nitrogen (99.999% purity) was utilized as the carrier gas at a flow rate of 1 ml/min. The ion source temperature was maintained at 250°C and a 70 eV electrode was used for ionization. Finally, the compounds were identified by comparison with the National Institute of Standards and Technology (NIST) mass spectra library.

X-Ray Powder Diffraction Analysis

The mineral composition of sediments was determined through XRD analysis at the Qinghai Institute of Salt Lake, Chinese Academy of Sciences (Xining, China), using an X Pert-PRO diffractometer (BRUKER, Germany) with a CuKα radiation source and a scanning speed of 0.02°/s. The applied voltage and tube currents were 45 kV and 30 mA, respectively.

Quantification of Total Organic Carbon

Quantification of total organic carbon (TOC) was performed as per the procedure previously reported by Wu et al. (2012), with some modifications. Briefly, 2 g of sample was treated with 20 ml of 1 mol/L hydrochloric acid, then washed with deionized water five times until the acid was removed and dried in a crucible at 900°C. The sample was ground to a powder using an element analyzer (Elementar, Germany) and decomposed at 950°C. Finally, the carbon mass percentage was determined.

n-Alkane Analysis

The salt lake sediments were subjected to two cycles of extraction using an accelerated solvent extractor (Dionex ASE 350, Thermo Scientific, United States) with dichloromethane/methanol (93:7) at 100°C and 1,600 psi. The *n*-alkane was separated using a deactivated silica gel column eluted with n-hexane. The *n*-alkane concentration was quantified using the GC-MS system (7890B/5977B, Agilent technologies, United States). The capillary column was an HP-5MS silica capillary column (30 m × 250 μm × 0.25 μm), coated with 5% phenyl methyl silox. The GC-oven temperature was initially 50°C (held for 1 min), then increased to 315°C (held for 16 min) at 8°C/min. Individual *n*-alkanes were identified and quantified by comparing with the spectra obtained using an alkane-mixture standard (C_{10}-C_{40}, Fluka, United States).

RESULTS

Mineralogy and Total Organic Carbon

The XRD spectra show that the mineral components in all samples were similar. Results indicate that the sediment samples were comprised of halite, quartz, albite, muscovite, gypsum, chlorite, calcite, aragonite, and dolomite (**Table 2**). However, the two different lithologic strata exhibited significant differences in the content of halite and detrital minerals (quartz, albite, and muscovite). SS strata samples exhibited the characteristics of low salinity and a high content of detrital minerals, while SB strata samples exhibited the opposite characteristics of high salinity and a low content of detrital minerals. Quartz was the most dominant detrital mineral in the SS strata (relative proportion of up to 41%), followed by muscovite and albite. In contrast, in the SB strata, quartz occurred at low concentrations and muscovite and albite were not detected.

Other than detrital minerals, samples also contained carbonate (calcite), sulfate (gypsum), silicate, and halite minerals. The content of silicate ranged from 72 to 84%. Sulfate was identified in all sediments, although the content of carbonate in SB strata was only 1%. Generally, the mineral components were more abundant in the SS strata than in the SB strata.

The TOC content of lake sediment samples is also presented in **Table 2**, exhibiting differences in the samples from different sediment strata. The TOC values ranged from 0.02 to 0.17%, with the TOC content of SS strata samples ranging from 0.12 to 1.17% (mean 0.14%), while that of SB strata ranged from 0.02 to 0.04% (mean 0.03%). The observed variation between strata may be attributed to the differences in environment conditions and external inputs during the formation of salt lake sediment layers.

Sediment Organic Matter Functional Groups

The FTIR spectra of samples from the same stratum exhibit similar patterns (**Figure 3**). FTIR spectra of samples from the SB strata exhibit a more complex range of characteristic adsorption peaks than SS strata samples, especially at the range of 2,000–400 cm^{-1}. The determination of spectral peaks was based on the characteristic peaks of relevant organic and

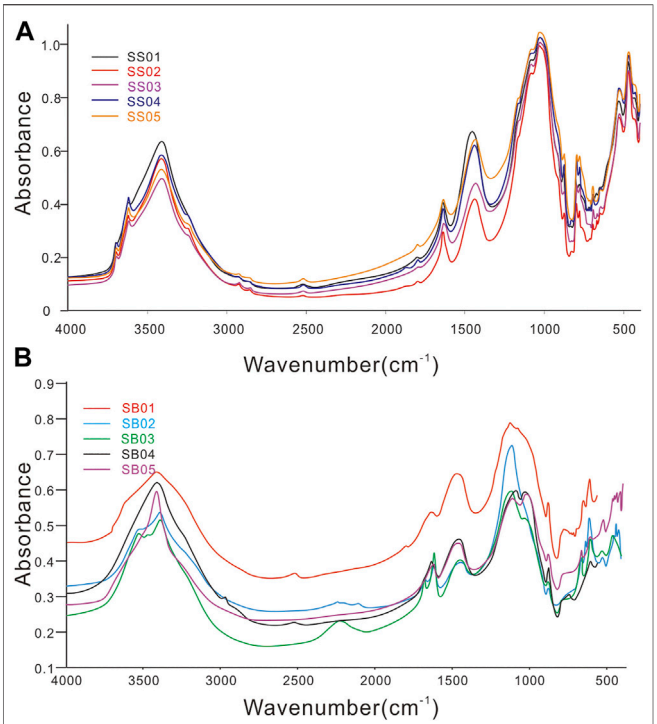

FIGURE 3 | FTIR spectra of different lithologic samples: **(A)** Silty sand; **(B)** Salt-bearing strata.

inorganic component functional groups, as reported in the literature (**Table 3**).

The absorbance band at 3,700–3,618 cm^{-1} corresponding to the stretching of O–H bonds in kaolinite (Rahier et al., 2000), with this band is only detected in SS. The absorption peak at 3,554–3,409 cm^{-1} was assigned to the stretching vibrations of O–H bonded hydroxyl groups of alcohols, phenols, and water molecules (Ellerbrock et al., 1999), as well as NH functional groups (Szymański, 2017). The absorption peaks at 2,936–2,847 cm^{-1} were assigned to asymmetric and symmetric stretching vibrations from aliphatic CH_2 groups (Dutta et al., 2013). The absorbance peaks at 1,869–1,678 cm^{-1} were attributed to the weak C=O stretching of conjugated ketones and anhydride (Coates, 2006), as well as to carboxylic acids and carbonyl bands in esters (Sarkhot et al., 2007), with these absorbance bands detected in all sediment samples from both lithologic strata. The bands in the region 1,645–1,620 cm^{-1} were attributed to the O–H bending modes of water (Ramasamy et al., 2009). The absorbance peak at 1,451–1,432 cm^{-1} was relatively complex, with Parolo et al. (2017) relating this peak to CO_3^{2-} vibrations in calcite and dolomite group minerals, or C–H bending vibrations of CH_3 and CH_2 groups. The band at 1,470 cm^{-1} was assigned as hydrogen-bonded O–C–O stretching of the carbonate ion (Oh et al., 2005). The peak in the range of 1,031–1,028 cm^{-1} may be related to the presence of OCH_3 or OH in alcohols (Rosa et al., 2016).

In addition to organic compounds, FTIR spectra also exhibited characteristic absorbance peaks for inorganic components. The absorbance band at 2,519–2,514 cm^{-1} was associated with the vibrations of CO_3^{2-} in calcite and dolomite group minerals. Generally, bands occurring below 1,000 cm^{-1} are related to a mixture of organic and inorganic compounds, such as quartz and clay minerals (Haberhauer et al., 2000; Calderón et al., 2013). The absorbance peak at 880–873 cm^{-1} was attributed to the same CO_3^{2-} vibrations as 2,519–2,514 cm^{-1}. The band in the range of 837–747 cm^{-1}, was assigned to Si–O–Si symmetrical stretching vibration in quartz (Lü et al., 2013). According to Ellerbrock et al. (1999), the band at 730–427 cm^{-1} was associated with inorganic components such as kaolinite, quartz, and gypsum.

Sediment Organic Matter Characterization by GC-MS

The characterization of SOM by GC-MS exhibited similar molecular compositions for both lithologic strata. The identified compounds included hydrocarbons, esters, aldehydes, ketones, furans, phenols, and alcohols. However, the proportions of these compounds in OM were significantly different. A total of twenty-five to thirty-four compound types were detected by GC-MS in SS, with phenols having the highest content, followed by hydrocarbons and aldehydes, while alcohols were only detected in sample SS02. The results are presented in detail in the supporting information (**Supplementary Table S1**).

Phenolic compounds are one of the most important secondary metabolites in plants (Karakaya, 2004), which are generally weakly acidic and easily oxidized in the environment. Four phenolic compounds were detected in SS strata samples, accounting for 25.09–55.73% of OM (mean proportion of 41.92%), most of which were diphenols.

Among the detected hydrocarbons, alkanes accounted for a distinctly larger proportion than other hydrocarbons. Alkanes are thought to be derived from lipid breakdown and are important biomarkers in geological analysis (Shanina, 2002; Fang et al., 2014). In total, between 10 and 17 hydrocarbons were identified in each SS strata sample, accounting for 29.33–56.02% of OM (mean proportion of 40.44%), with the second highest abundance after phenols. However, among all the identified compounds, hydrocarbons accounted for the most compound types.

The content of aldehyde compounds in SS strata samples ranged from 3.47 to 19.24% of OM (mean proportion of 10.19%). Among all the detected aldehydes, the average proportion of nonanal was highest. It is well established, that nonanal is an oxidative catabolite of fatty acids (Yang et al., 2008). Therefore, the high proportion of nonanal throughout the sediment depth profile indicates periods of intense vegetation (Dąbrowska et al., 2014).

The esters detected in SS strata samples are mainly methyl, butyl, and amyl esters, accounting for 3.34–11.41% of OM (mean proportion of 6.85%). Two ketones were identified, include 3-heptanone and methylheptenone. Ketones primarily result from amino acid degradation (Zhuang et al., 2016), with amino acids being the main protein units present in all living organisms. 2-pentylfuran was the only furanoic compound detected in all SS strata samples, accounting for 0.07–0.55% of OM (mean proportion of 0.18%). Alcohols were only detected in sample DP02, including 1-octanol and 2-ethyl-1-hexanol, with an abundance of 1.23%.

A total of thirty-six to forty-five kinds of compounds were detected in SB strata samples. Aldehydes (31.41–66.87%, mean

proportion of 48.65%) exhibited the highest abundance, followed by hydrocarbons (16.25–40.61%, mean proportion of 26.19%), esters (4.78–16.31%, mean proportion of 10.42%), phenols (3.45–8.18%, mean proportion of 8.66%), ketones (1.88–5.53%, mean proportion of 2.28%), and alcohols (0.05–0.34%, mean proportion of 0.15%). The results are summarized in detail in the supporting information (**Supplementary Table S2**).

n-Alkanes in Sediments

n-Alkanes with carbon numbers between C_{15} and C_{36} were found in all samples (**Figure 4**). Short-chain *n*-alkanes (C_{15}–C_{20}) were less abundant, with relative abundances varying from 1.15 to 8.61%, with an average content of 3.51%. The abundance of mid-chain *n*-alkanes (C_{21}–C_{25}) varied from 9.37 to 35.99%, with an average content of 24.54%. In contrast, the long-chain *n*-alkanes (C_{26}–C_{36}) were highly abundant in all sediments, ranging from 53.25 to 83.99%, with an average content of 69.83%. In SB sediments, the carbon maximum (C_{max}) of long-chain *n*-alkanes occurred at C_{31}, while for SS sediments, the C_{max} occurred at C_{25} and C_{27}. The carbon preference index (CPI) values in SB sediments varied from 3.79 to 11.02 (avg 6.72), the Pristane/Phytane (Pr/Ph) values varied from 0.23 to 0.83 (avg 0.41), and the Pr/nC_{17} and Pr/nC_{18} values varied from 1.03 to 1.62 (avg 1.35) and 0.98–1.17 (avg 1.11), respectively. In SS sediments, the CPI values varied from 1.22 to 1.53 (avg 1.31), the Pr/Ph values varied from 0.26 to 0.44 (avg 0.38), and the Pr/nC17 and Pr/nC18 values varied from 0.70 to 1.54 (avg 1.16) and 1.20–1.87 (avg 1.46), respectively.

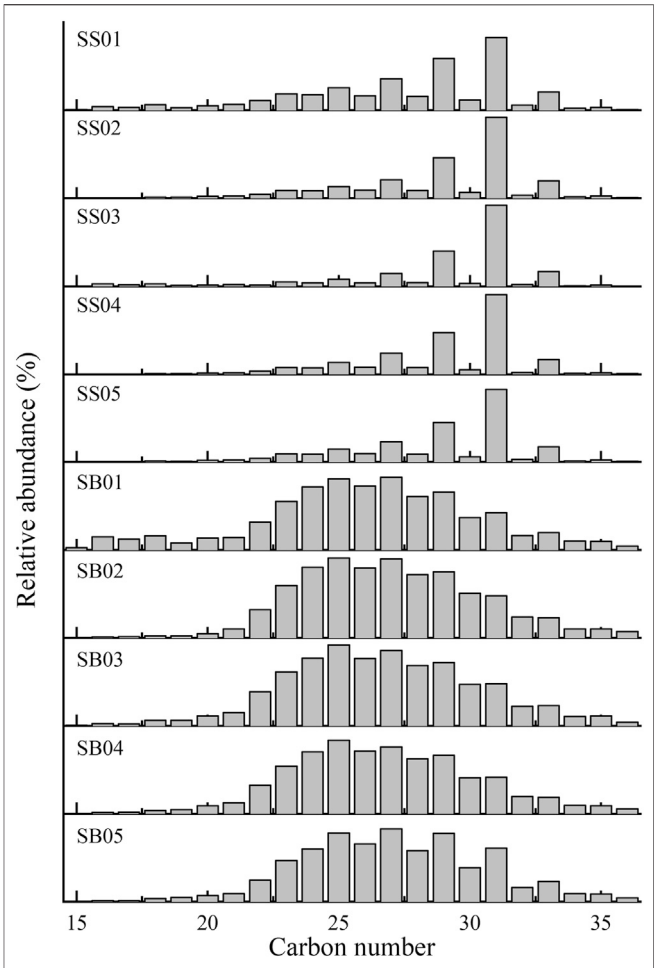

FIGURE 4 | Distribution of *n*-alkanes in different lithologic strata of salt lake sediments.

DISCUSSION

FTIR Analysis of Sediment Organic Matter

The identified FTIR absorbance bands from sediments in the same stratum exhibited identical peak positions and comparable absorbance intensities, indicating a similar molecular composition of SOM. This observation is in agreement with the previously reported results of Giovanela et al. (2010) and Pongpiachan et al. (2013) who found similar molecular compositions of SOM from within the same stratum or the same area. In the present study, several similar peak positions were found to exist in both strata, confirming that the same organic matter was present in different strata.

TABLE 3 | FTIR spectra band positions observed in the present study and reported in previous literature.

Peak position (cm^{-1})		Proposed assignment
Current study	**Literature**	
3,700–3,618	3,700–3,600	Stretching of O–H bond in kaolinite (Omar et al., 2020)
3,554–3,404	3,600–3,400	Stretching of O–H bond in water, carboxyl, and hydroxyl groups (Somani et al., 2003)
2,926–2,847	3,000–2,800	The aliphatic CH_2 stretching vibration (Yu et al., 2007)
2,519–2,514	2,515	Vibrations of CO_3^{2-} in calcite and minerals of the calcite and dolomite groups (So et al., 2020)
1,869–1,678	1,870–1,675	C=O stretching of conjugated ketones and anhydride (Coates, 2006)
1,645–1,620	1,650–1,600	O–H bending modes of water or hydroxyls (Cocozza et al., 2003)
1,451–1,432, 1,471	1,450–1,430, 1,470	C–H bending vibrations of CH_2 and CH_3 groups and vibrations of CO_3^{2-} in calcite, O–C–O stretching of the carbonate ion (Parolo et al., 2017)
1,168–1,078	1,116–1,080	Secondary alcohols (Laudicina et al., 2015)
1,031–1,028	1,080–1,030	Vibrations of OCH_3 as well as OH in alcohols (Senesi et al., 2003)
880–873	887–866	Vibrations of CO_3^{2-} in calcite and minerals of the calcite and dolomite groups (So et al., 2020)
837–747	830–750	Si–O–Si symmetrical stretching vibration (Hao, 2001)
730–427	800–400	Inorganic components (such as kaolinite, quartz, and gypsum) (Ellerbrock et al., 1999)

Despite the broad similarities in SOM chemical composition between the two different lithologic strata, there were significant differences observed in the relative abundance of certain C functional groups and distribution trends within strata. Compared with SS strata, five sediments of SB strata generally exhibited a higher content of ketone C=O groups (1,869–1,678 cm^{-1}) and a lower content of aliphatic C (2,926–2,847 cm^{-1}), with an equal abundance of alcohols (1,168–1,078 cm^{-1} and 1,031–1,028 cm^{-1}) (**Figure 3**). The enrichment of aliphatic C forms in SS strata may be associated with a more advanced stage of OM decomposition (Omar et al., 2020), with the persistence of aliphatic C groups during decomposition suggesting that it may represent relatively stable and recalcitrant forms of C in sediments (Lorenz et al., 2007; Calderón et al., 2011). Therefore, OM and the microorganisms that can decompose OM should be more abundant in SS than in SB strata. A lower abundance of ketone C=O groups (1,869–1,678 cm^{-1}) was observed in SS strata. According to Ndwigah et al. (2013), ketones are mainly produced by halophilic fungi, supporting the theory that the SB layer was deposited in an arid climate under increased salinity conditions. Alcohols exist widely in organisms and sediments, and the genesis of alcohols in sediments is extremely complex, which not only depends on the source of OM, but is also affected by many factors such as biochemistry and geochemistry (Duan et al., 1995). Previous studies on the genesis of alcohols have been based on characteristic organisms and different sedimentary environments, with the main influencing factors including either alga (Robinson et al., 1986; Nichols et al., 1990) or terrestrial organic matter (Volkman et al., 1987; Goossens et al., 1989). This result explains why the alcohol content of the different strata is almost the same, despite the SS sedimentary environment being different from that of SB strata.

Furthermore, the SS strata exhibited an abundance of characteristic peaks for carbonate (2,519–2,514 cm^{-1}, 1,451–1,432 cm^{-1}, 1,471 cm^{-1}, and 880–873 cm^{-1}) and detrital minerals (730–427 cm^{-1}). According to Keil et al. (1994), OM is associated with mineral grains, which subsequently reduces the rate of decomposition (Wang and Lee, 1993), with OM primarily filling the mineral pores of quartz aggregates, forming OM networks (Zhao et al., 2017b). Detrital minerals are mainly composed of quartz, sodium feldspar and muscovite, with these compounds serving a significant role in the diagenetic process and reflecting extrabasinal and intrabasinal sediment inputs (Zhao et al., 2017a). In general, detrital minerals come from peripheral areas of the lake and are supplied by processes including surface run-off, river transport, atmospheric rainfall, and lakeshore erosion (Shen et al., 2010). In humid climates, increased precipitation promotes surface run-off, carrying the insoluble detrital minerals into the salt lake and depositing them directly on the bottom of the lake bed. As a result, the paleoclimate appears to be warmer and wetter after 4 ka BP, with the exogenous OM and TOC content in SS strata being higher than in SB strata.

SOM Analysis by GC-MS

GC-MS analysis showed that the molecular types OM in different lithologic strata are relatively similar, with the identified substances classified into seven types, including aldehydes, hydrocarbons, phenols, esters, ketones, alcohols, and furans. The proportional abundances of different types of OM in different lithologic strata are shown in **Figure 5**.

Different strata have different distributions of organic molecular types. SS strata contain the highest content of phenolic substances, while the content of hydrocarbons is close to that of phenolic substances, with the total content of the two substances being more than 80%. The main sources of phenols in sediments are root exudates, microbial secretions, and plant tissue decomposition (Bao et al., 2013a, 2013b; Vane et al., 2013), while hydrocarbons are affected by many factors such as organic source, microbial activity, and the redox environment (Wu et al., 2001). In view of the particular characteristics of salt lake sediments, exogenous OM and microbial communities significantly contribute to the OM content in SS strata. In SB strata, the content of aldehydes accounts for almost half of the OM. In high salinity environments, aldehydes are mainly produced by algae (such as diatoms) (; Chen et al., 2014a; Chen et al., 2014b) and therefore, the main contributor to OM in SB strata is likely to be algae.

In general, according to the sedimentary characteristics of the salt lake, the environmental conditions of SB strata during the sedimentary period are more extreme than for SS strata (Shen et al., 2010). However, more organic compounds were identified in SB strata (mean of 41 compounds) than in SS strata (mean of 30 compounds). This observation is partially supported by a previous study showing that the higher salinity of halite may affect the enrichment of some organic compounds (Strehse et al., 2018). Higher salinity also results in stratification of the water column, creating an anoxic sedimentary environment and inhibiting bacterial proliferation (Zhu et al., 2004), thereby reducing the consumption of OM. Klinkhammer and Lambert (1989) presented evidence for organic carbon preservation in high salinity sediments, while Jellison et al. (1996) reported a positive correlation between the accumulation of organic carbon and salinity levels. Overall, these phenomena may be attributed to the specific characteristics of sediment layers, such as salinity and biological composition.

The main differences in OM between the two strata layers are the proportions of phenols and aldehydes (**Figure 6**). The proportion of phenols in the SS strata was much larger than in the SB strata, while the proportion of aldehydes in the SB strata was higher than in the SS strata. Many organisms have developed protective mechanisms allowing phenol to be used as their sole carbon and energy source (Schie and Young, 2000). Thus, the degradation of phenols by halophilic bacteria in high salinity environments is of relevance (Peyton et al., 2002; Li et al., 2019). Haddadi and Shavandi (2013) reported a Halomonas sp. strain that exhibited the ability to utilize phenol as the sole carbon and energy source in saline environments. Preliminary evidence has been reported that indicates that phenol degradation proceeds in some halophilic bacteria through a *meta*-cleavage pathway (Acikgoz and Ozcan, 2016). The survival and activity of halophilic bacteria are better suited to the environment of SB strata than SS strata, leading to more phenol degradation in SB strata. This phenomenon also results in a larger reduction in the

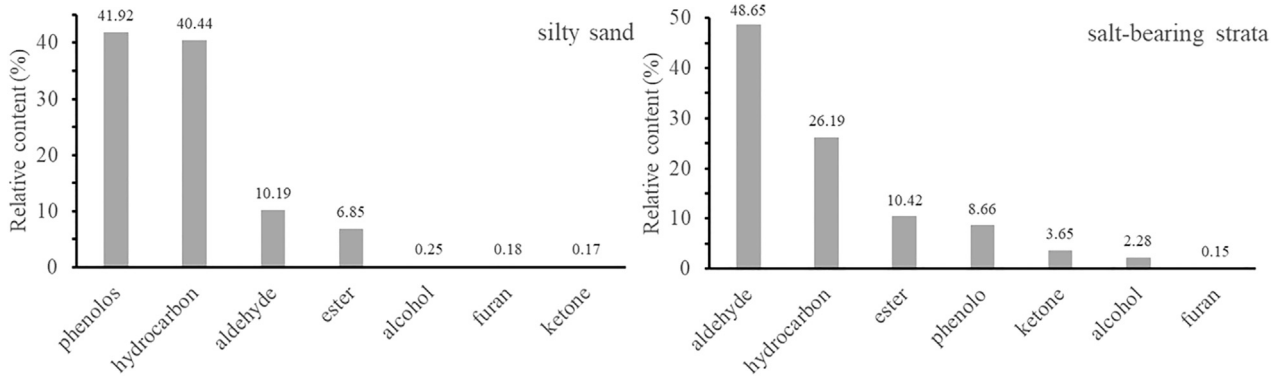

FIGURE 5 | Organic matter content in different lithologic strata.

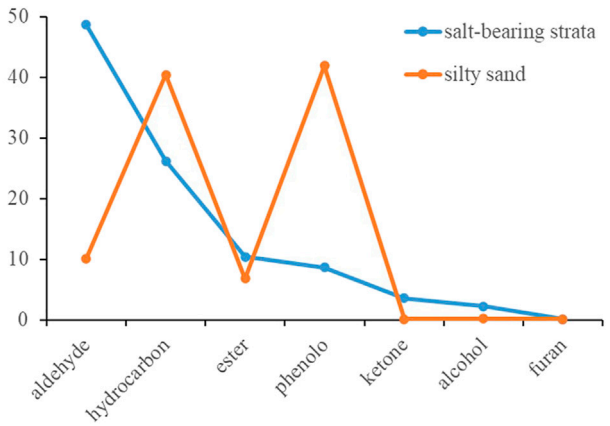

FIGURE 6 | Differences in the distribution of organic matter in different lithologic strata.

proportion of phenols in SB strata. In addition, it further confirms that the paleoclimate of 4 ka BP appears to have been more extreme and that phenols may be a potential biomarker for reconstruction of the paleoclimate in this period. This is partially supported by a previous study showing that lignin phenol can be used as a biomarker for paleovegetation in soils (Kovaleva and Kovalev, 2015).

Algae are another main producer of OM in high salinity environments, with a large number of aldehydes produced at the same time. Especially in the later stage of diatom growth, the content of aldehydes continues to increase, with previous studies reporting that the content of aldehydes can reach up to 46.8% of the total volatile fraction (Chen et al., 2014a). In a previous study on nine kinds of diatoms, Chen et al. (2014a) found that nonanal was dominant among the volatile aldehydes of diatoms in the later stage of sedimentation. This result corresponds to the observed content of nonanal in the present study. Therefore, it may be inferred that the higher content of aldehydes in the SB strata occurs mainly due to the higher abundance of diatoms in salt lake water during the sedimentary period, as compared to SS. The aldehyde content also confirmed that the paleoclimate around 4 ka BP changed from cold and dry to relatively warm and wet.

Correlation Analysis Between Mineral Composition and Organic Matter

In this study, correlation analysis was performed between detrital minerals and various types of OM in all samples (**Table 4**). Results show a strong positive correlation between detrital minerals and phenols, with a strong negative correlation between detrital minerals and aldehydes, which was consistent with the results of GC-MS and XRD analysis. However, a negative correlation between detrital minerals and ketones was observed. According to Schmidt et al. (2015), most volatile OM components are considered to be side products of primary and secondary metabolism, with ketones produced by bacteria or fungi (Piechulla and Degenhardt, 2014). These findings agree with the results of a previous study, showing that some halophilic fungal species in salt lakes were able to produce a wide range of secondary metabolites such as ketones (Ndwigah et al., 2013). Therefore, it can be preliminarily determined that the production of ketones in this study may be closely related to some halophilic fungi in lake sediments, indicating that ketones should be produced in large quantities in salt lakes under arid climate conditions.

OM is always associated with mineral grains (Keil et al., 1994) in lake sediments and due to the high salinity in salt lake sediments, OM is mainly formed by microorganisms (Han et al., 2020) and algae (Meyers and Ishiwatari, 1993). Detrital minerals serve a significant role in the diagenetic process and reflect extrabasinal and intrabasinal sediment inputs in salt lake environments (Zhao et al., 2017b). In general, detrital minerals originate from peripheral areas of the lake and are supplied by processes including surface run-off, river transport, atmospheric rainfall, and lakeshore erosion (Shen et al., 2010). In humid climates, increased precipitation levels promote higher levels of surface run-off, carrying insoluble detrital minerals into the lake and depositing them directly on the bottom of the salt lake. This spatial distribution of detrital mineral in sediments shows that the preferential feeding areas correspond to SS in our study. The high

TABLE 4 | Correlation analysis between clastic rocks and organic matter.

	Detrital minerals	Aldehydes	Hydrocarbons	Esters	Phenols	Ketones	Alcohols	Furans
Detrital minerals	1	–0.863**	0.574	–0.394	0.899**	–0.704*	–0.618	0.070
Aldehydes		1	–0.745*	0.186	–0.877**	0.670*	0.285	0.009
Hydrocarbons			1	–0.271	0.414	–0.681*	–0.123	0.388
Esters				1	–0.380	0.653*	0.299	0.226
Phenols					1	–0.681*	–0.471	–0.266
Ketones						1	0.457	–0.090
Alcohols							1	–0.383
Furans								1

*Note: *p ≤ 0.05, significant correlation; **p ≤ 0.01, extremely significant correlation.*

abundances of quartz and feldspar in the sediments reveal a period of active detrital input. Wirrmann et al. (2001) demonstrated that detrital mineral flux can be used as a proxy indicator for the mean rainfall intensity and based on this, precipitation during SS deposition was higher than during SB deposition. Furthermore, the content of detrital minerals increases while salinity is simultaneously reduced, which is consistent with the results of XRD analysis in the present study. This conclusion is supported by Yang (2015) who reported the occurrence of frequent catastrophic floods by the Nalinggele River during the 4.7–3.5 ka BP period.

The correlation between mineral composition and OM in the sediments of East Taijinar salt lake, demonstrates that the concentrations of aldehydes and ketones were relatively high due to the dry climate during the period of deposition and the relative development of halophilic algae in the lake prior to 4 ka BP. However, with adaptation of the climate to warm and humid conditions, a large amount of exogenous OM was imported, resulting in a relative increase in the phenol content after 4 ka BP. Meanwhile, the detrital mineral flux in different strata also confirmed that the paleoclimate had changed from dry and cool to warm and wet in the 4 ka BP period.

Further Verification of Paleoclimate Changes Around 4 ka BP Using the Content of *n*-Alkanes

n-Alkanes in sediments mainly originate from fatty acids and waxes in organism cells (Sachse et al., 2004), serving as widely studied biomarkers that are widely distributed in soils (Wang et al., 2007), loess deposit (Zeng et al., 2011), and lacustrine deposits. Bacteria and algae produce both odd and even carbon number short-chain *n*-alkanes (Meyers, 2003), while the abundance of odd long-chain *n*-alkanes (C_{27}–C_{31}) has been extensively utilized as an indicator of terrestrial or land-derived OM (Pearson and Eglinton, 2000; Zhao et al., 2003). In the present study, the SS sediments samples exhibited an odd-over-even predominance and were mainly dominated by C_{31}, while SB sediment samples were dominated by C_{25} and C_{27} without an odd-over-even predominance. This result is in agreement with a previous study showing that long-chain *n*-alkanes can also be produced by bacteria and algae, although these long-chain *n*-alkanes do not exhibit an odd-even dominance (Castañeda and Schouten, 2011).

The nC_{31}/nC_{29} ratio of *n*-alkanes in sediments is often used as an indicator of environmental and paleoclimate change (Meyers and Ishiwatari, 1993). It has been shown that nC_{31} is the main *n*-alkanes peak in herbaceous plants, while nC_{29} is the main *n*-alkanes peak in woody plants. When herbaceous plants are dominant, the climate tends to be warm and humid, resulting in nC_{31} being the main *n*-alkane compound; when woody plants are dominant, the climate tends to be cold and dry, resulting in *n*-alkanes being dominated by nC_{29} (Cranwell, 1973; De las Heras et al., 1989). Therefore, $nC_{31}/nC_{29} > 1.0$ indicates that the climatic environment in this period was relatively warm and humid, while $nC_{31}/nC_{29} < 1.0$ reflects that the climatic environment was cold and dry. The established nC_{31}/nC_{29} ratios are presented in **Figure 2**, with the ratio of nC_{31}/nC_{29} ranging from 0.64 to 0.79 in SB, while the values were >1.0 (1.41–2.31) in SS sediments. Therefore, the paleoclimate around 4 ka BP during the sedimentary period ranging from SB to SS, changed from dry and cool to warm and wet.

Furthermore, CPI values > 1.0 indicate terrestrial OM inputs (Bray and Evans, 1961). The CPI values in SS sediments ranged from 3.79 to 11.02 (avg 6.72), demonstrating that the main source of OM appears to be terrestrial in SS sediments. The Pr/Ph, Pr/C_{17}, and Pr/C_{18} values are presented in **Figure 2**. The Pr/Ph ratio is used in a lacustrine setting to infer the oxic vs anoxic state during OM deposition, with Pr/Ph ratios <1.0 indicating anoxic conditions, whereas values > 1.0 reflect suboxic to oxic environments (Didyk et al., 1978). The Pr/Ph value of East Taijinar salt lake sediments from around the 4 ka BP period, suggest that deposition occurred under anoxic conditions due to the overlying lake water. It has been reported that Pr/nC_{17} and Pr/nC_{18} values of OM without degradation are very low (0.1–0.5), while higher values occur when OM is degraded by microorganisms (Zhao et al., 2016). In the present study, the ratio of Pr/nC17 (0.70–1.62 avg 1.26) and Pr/nC18 (0.98–1.87 avg 1.28) indicate strong microbial activities in East Taijinar salt lake sediments around the 4 ka BP period.

These findings indicate that the OM in SS sediments was mainly terrestrial OM, while the OM in SB sediments could have a bacterial and algal source. The paleoclimate of the SB deposition period appears to be drier than that of SS deposition period, with the climate becoming warmer after the 4 ka BP period. Furthermore, the OM in all sediment samples was found to be strongly affected by microorganisms in anoxic environments, which is consistent with the results on OM distribution

characteristics, further confirming the importance of OM in paleoclimate change.

CONCLUSION

This study preliminarily investigates the spectral characteristics and volatile organic composition of East Taijinar salt lake sediments around 4 ka BP. XRD, FTIR, and GC-MS analysis enabled the characterization of sediment OM. The TOC concentration was significantly lower in SB strata than SS strata, which may be attributed to environmental differences during the formation of salt lake sediments. FTIR spectroscopy showed a relative enrichment of ketone C=O groups in SB strata, and a decrease in aliphatic C compared with the SS strata. These findings are confirmed by the results of GC-MS analyses and the relationship between OM and detrital minerals. The high content of phenols in the SS strata indicates that the organic sources and microorganisms contribute greatly to the OM content of SS, with the paleoenvironment likely being warm and humid. The high content of aldehydes in SB strata indicates a high abundance of diatoms in the salt lake water during the sedimentation period, with the climate likely to be relatively dry and cool at that time. Correlation analysis showed a strong positive correlation between detrital minerals and phenols, while a strong negative correlation was observed between detrital minerals and aldehydes, and a negative correlation was also observed between detrital minerals and ketones. The correlation analysis results indicate that OM in SS sediments is strongly affected by exogenous organic inputs, with the detrital mineral flux in different strata further confirming that the climate had changed from cool and dry, to wet and warm at 4 ka BP. The analysis of *n*-Alkanes in sediments, provides a tool to sensitively monitor paleoclimate changes in the middle area of the QB around the 4 ka BP period. Overall, the dominant carbon number, nC_{31}/nC_{29} ratio and CPI values all indicate that the climate changed from dry to warm, confirming that the spectral characteristics and content of VOCs in salt lake sediments are related to paleoclimate changes.

DATA AVAILABILITY STATEMENT

The original contributions presented in the study are included in the article/**Supplementary Material**, further inquiries can be directed to the corresponding authors.

AUTHOR CONTRIBUTIONS

ZM and XL performed the fieldwork; YZ and LY performed laboratory analysis; XL and LY prepared the figures and tables; XL, YZ, and FH wrote the manuscript with the help of all co-authors.

FUNDING

This work was supported by the Natural Science Foundation of Qinghai Province (2019-ZJ-911).

ACKNOWLEDGMENTS

We thank YZ for her assistance with the experiment and data analysis. We also thank Yixuan Wang, who helped with sample dating.

SUPPLEMENTARY MATERIAL

The Supplementary Material for this article can be found online at: https://www.frontiersin.org/articles/10.3389/feart.2021.734458/full#supplementary-material

REFERENCES

Acikgoz, E., and Ozcan, B. (2016). Phenol Biodegradation by Halophilic Archaea. *Int. Biodeterioration Biodegradation* 107, 140–146. doi:10.1016/j.ibiod.2015.11.016

Aichner, B., Herzschuh, U., Wilkes, H., Schulz, H.-M., Wang, Y., Plessen, B., et al. (2012). Ecological Development of Lake Donggi Cona, north-eastern Tibetan Plateau, since the Late Glacial on Basis of Organic Geochemical Proxies and Non-pollen Palynomorphs. *Palaeogeogr. Palaeoclimatol. Palaeoecol.* 313-314, 140–149. doi:10.1016/j.palaeo.2011.10.015

An, Z., Colman, S. M., Zhou, W., Li, X., Brown, E. T., Jull, A. J. T., et al. (2012). Interplay between the Westerlies and Asian Monsoon Recorded in Lake Qinghai Sediments since 32 Ka. *Sci. Rep.* 2, 619. doi:10.1038/srep00619

Bao, H., Wu, Y., Tian, L., Zhang, J., and Zhang, G. (2013a). Sources and Distributions of Terrigenous Organic Matter in a Mangrove Fringed Small Tropical Estuary in South China. *Acta Oceanol. Sin.* 32, 18–26. doi:10.1007/s13131-013-0295-3

Bao, H., Wu, Y., Unger, D., Du, J., Herbeck, L. S., and Zhang, J. (2013b). Impact of the Conversion of Mangroves into Aquaculture Ponds on the Sedimentary Organic Matter Composition in a Tidal Flat Estuary (Hainan Island, China). *Continental Shelf Res.* 57, 82–91. doi:10.1016/j.csr.2012.06.016

Bray, E. E., and Evans, E. D. (1961). Distribution of N-Paraffins as a Clue to Recognition of Source Beds. *Geochimica et Cosmochimica Acta* 22, 2–15. doi:10.1016/0016-7037(61)90069-2

Brown, G. E., and Calas, G. (2012). Mineral-aqueous Solution Interfaces and Their Impact on the Environment. *Geochem. Perspect.* 1, 483–484. doi:10.1016/j.scitotenv.2020.140292

Calderón, F., Haddix, M., Conant, R., Magrini-Bair, K., and Paul, E. (2013). Diffuse-Reflectance Fourier-Transform Mid-infrared Spectroscopy as a Method of Characterizing Changes in Soil Organic Matter. *Soil Sci. Soc. America J.* 77, 1591–1600. doi:10.2136/sssaj2013.04.0131

Calderón, F. J., Reeves, J. B., Collins, H. P., and Paul, E. A. (2011). Chemical Differences in Soil Organic Matter Fractions Determined by Diffuse-Reflectance Mid-infrared Spectroscopy. *Soil Sci. Soc. Am. J.* 75, 568–579. doi:10.2136/sssaj2009.0375

Castañeda, I. S., and Schouten, S. (2011). A Review of Molecular Organic Proxies for Examining Modern and Ancient Lacustrine Environments. *Quat. Sci. Rev.* 30, 2851–2891. doi:10.1016/j.quascirev.2011.07.009

Chen, F., Wu, D., Chen, J., Zhou, A., Yu, J., Shen, J., et al. (2016). Holocene Moisture and East Asian Summer Monsoon Evolution in the Northeastern Tibetan Plateau Recorded by Lake Qinghai and its Environs: A Review of Conflicting Proxies. *Quat. Sci. Rev.* 154, 111–129. doi:10.1016/j.quascirev.2016.10.021

Chen, F., Yu, Z., Yang, M., Ito, E., Wang, S., Madsen, D. B., et al. (2008). Holocene Moisture Evolution in Arid central Asia and its Out-of-phase Relationship with Asian Monsoon History. *Quat. Sci. Rev.* 27, 351–364. doi:10.1016/j.quascirev.2007.10.017

Chen, J., Xu, J., Li, Y., Zhou, C., and Yan, X. (2014a). Analysis of Volatile Components from Three marine Diatoms at Different Growth Stages. *Acta Oceanol. Sin.* 36, 49–64. doi:10.3969/j.issn.2095-736.2014.02.035

Chen, J., Xu, J., Li, Y., Zhou, C., and Yan, X. (2014b). Comparative Analysis of Volatile Components in Nine Species of marine Diatoms. *J. Biol.* 31, 35–40. doi:10.3969/j.issn.0253-4193.2014.05.006

Cheng, B., Chen, F., and Zhang, J. (2013). Palaeovegetational and Palaeoenvironmental Changes since the Last Deglacial in Gonghe Basin, Northeast Tibetan Plateau. *J. Geogr. Sci.* 23, 136–146. doi:10.1007/s11442-013-0999-5

Coates, J. (2006). "Interpretation of Infrared Spectra, A Practical Approach," in *Encyclopedia of Analytical Chemistry* (New York: American Cancer Society). doi:10.1002/9780470027318.a5606

Cocozza, C., D'Orazio, V., Miano, T. M., and Shotyk, W. (2003). Characterization of Solid and Aqueous Phases of a Peat Bog Profile Using Molecular Fluorescence Spectroscopy, ESR and FT-IR, and Comparison with Physical Properties. *Org. Geochem.* 34, 49–60. doi:10.1016/s0146-6380(02)00208-5

Cranwell, P. A. (1973). Chain-length Distribution of N-Alkanes from lake Sediments in Relation to post-glacial Environmental Change. *Freshw. Biol* 3, 259–265. doi:10.1111/j.1365-2427.1973.tb00921.x

De las Heras, X., Grimalt, J. O., Albaigés, J., Juliá, R., and Anadon, P. (1989). Origin and Diagenesis of the Organic Matter in Miocene Freshwater Lacustrine Phosphates (Cerdanya Basin, Eastern Pyrenees). *Org. Geochem.* 14, 667–677. doi:10.1016/0146-6380(89)90046-6

Derenne, S., and Quénéa, K. (2015). Analytical Pyrolysis as a Tool to Probe Soil Organic Matter. *J. Anal. Appl. Pyrolysis* 111, 108–120. doi:10.1016/j.jaap.2014.12.001

Didyk, B. M., Simoneit, B. R. T., Brassell, S. C., and Eglinton, G. (1978). Organic Geochemical Indicators of Palaeoenvironmental Conditions of Sedimentation. *Nature* 272, 216–222. doi:10.1038/272216a0

Duan, Y., Luo, B., and Chen, N. (1995). Origin of Alcohol Compounds in Marine Sediments of Nansha. *Acta Oceanol. Sin.* 17, 123–127.

Dutta, S., Hartkopf-Fröder, C., Witte, K., Brocke, R., and Mann, U. (2013). Molecular Characterization of Fossil Palynomorphs by Transmission Micro-FTIR Spectroscopy: Implications for Hydrocarbon Source Evaluation. *Int. J. Coal Geology.* 115, 13–23. doi:10.1016/j.coal.2013.04.003

Dąbrowska, A., Nawrocki, J., and Szeląg-Wasielewska, E. (2014). Appearance of Aldehydes in the Surface Layer of lake Waters. *Environ. Monit. Assess.* 186, 4569–4580. doi:10.1007/s10661-014-3720-y

Ellerbrock, R. H., Höhn, A., and Rogasik, J. (1999). Functional Analysis of Soil Organic Matter as Affected by Long-term Manurial Treatment. *Eur. J. Soil Sci.* 50, 65–71. doi:10.1046/j.1365-2389.1999.00206.x

Ene, A., Bogdevich, O., Sion, A., and Spanos, T. (2012). Determination of Polycyclic Aromatic Hydrocarbons by Gas Chromatography-Mass Spectrometry in Soils from Southeastern Romania. *Microchemical J.* 100, 36–41. doi:10.1016/j.microc.2011.08.006

Fan, J., Xiao, J., Wen, R., Zhang, S., Wang, X., Cui, L., et al. (2017). Carbon and Nitrogen Signatures of Sedimentary Organic Matter from Dali Lake in Inner Mongolia: Implications for Holocene Hydrological and Ecological Variations in the East Asian Summer Monsoon Margin. *Quat. Int.* 452, 65–78. doi:10.1016/j.quaint.2016.09.050

Fang, J., Wu, F., Xiong, Y., Li, F., Du, X., An, D., et al. (2014). Source Characterization of Sedimentary Organic Matter Using Molecular and Stable Carbon Isotopic Composition of N-Alkanes and Fatty Acids in Sediment Core from Lake Dianchi, China. *Sci. Total Environ.* 473-474, 410–421. doi:10.1016/j.scitotenv.2013.10.066

Giovanela, M., Crespo, J. S., Antunes, M., Adamatti, D. S., Fernandes, A. N., Barison, A., et al. (2010). Chemical and Spectroscopic Characterization of Humic Acids Extracted from the Bottom Sediments of a Brazilian Subtropical Microbasin. *J. Mol. Struct.* 981, 111–119. doi:10.1016/j.molstruc.2010.07.038

Goossens, H., Düren, R. R., de Leeuw, J. W., and Schenck, P. A. (1989). Lipids and Their Mode of Occurrence in Bacteria and Sediments-II. Lipids in the Sediment of a Stratified, Freshwater lake. *Org. Geochem.* 14, 27–41. doi:10.1016/0146-6380(89)90016-8

Haberhauer, G., Feigl, B., Gerzabek, M. H., and Cerri, C. (2000). FT-IR Spectroscopy of Organic Matter in Tropical Soils: Changes Induced through Deforestation. *Appl. Spectrosc.* 54, 221–224. doi:10.1366/0003702001949131

Haddadi, A., and Shavandi, M. (2013). Biodegradation of Phenol in Hypersaline Conditions by Halomonas Sp. Strain PH2-2 Isolated from saline Soil. *Int. Biodeterioration Biodegradation* 85, 29–34. doi:10.1016/j.ibiod.2013.06.005

Hakim, S. S., Olsson, M. H. M., Sørensen, H. O., Bovet, N., Bohr, J., Feidenhans'l, R., et al. (2017). Interactions of the Calcite {10.4} Surface with Organic Compounds: Structure and Behaviour at Mineral – Organic Interfaces. *Sci. Rep.* 7, 7592. doi:10.1038/s41598-017-06977-4

Han, R., Zhu, D., Xing, J., Li, Q., Li, Y., and Chen, L. (2020). The Effect of Temperature Fluctuation on the Microbial Diversity and Community Structure of Rural Household Biogas Digesters at Qinghai Plateau. *Arch. Microbiol.* 202, 525–538. doi:10.1007/s00203-019-01767-0

Hao, B. (2001). IR Analysis of the Chemical Bond Changes in Quartz Powder during Superfine Milling. *Min. Metall. Eng.* 21, 64–66.

Isaji, Y., Kawahata, H., Ogawa, N., Kuroda, J., Yoshimura, T., Jiménez-Espejo, F. J., et al. (2019). Efficient Recycling of Nutrients in Modern and Past Hypersaline Environments. *Sci. Rep.* 9, 1–12. doi:10.1038/s41598-019-40174-9

Jellison, R., Anderson, R. F., Melack, J. M., and Heil, D. (1996). Organic Matter Accumulation in Sediments of Hypersaline Mono Lake during a Period of Changing Salinity. *Limnol. Oceanogr.* 41, 1539–1544. doi:10.4319/lo.1996.41.7.1539

Karakaya, S. (2004). Bioavailability of Phenolic Compounds. *Crit. Rev. Food Sci. Nutr.* 44, 453–464. doi:10.1080/10408690490886683

Keil, R. G., Tsamakis, E., Fuh, C. B., Giddings, J. C., and Hedges, J. I. (1994). Mineralogical and Textural Controls on the Organic Composition of Coastal marine Sediments: Hydrodynamic Separation Using SPLITT-Fractionation. *Geochimica et Cosmochimica Acta* 58, 879–893. doi:10.1016/0016-7037(94)90512-6

Kleber, M., Sollins, P., and Sutton, R. (2007). A Conceptual Model of Organo-mineral Interactions in Soils: Self-Assembly of Organic Molecular Fragments into Zonal Structures on mineral Surfaces. *Biogeochemistry* 85, 9–24. doi:10.1007/s10533-007-9103-5

Klinkhammer, G. P., and Lambert, C. E. (1989). Preservation of Organic Matter during Salinity Excursions. *Nature* 339, 271–274. doi:10.1038/339271a0

Kovaleva, N. O., and Kovalev, I. V. (2015). Lignin Phenols in Soils as Biomarkers of Paleovegetation. *Eurasian Soil Sci.* 48, 946–958. doi:10.1134/s1064229315090057

Laudicina, V. A., Novara, A., Barbera, V., Egli, M., and Badalucco, L. (2015). Long-Term Tillage and Cropping System Effects on Chemical and Biochemical Characteristics of Soil Organic Matter in a Mediterranean Semiarid Environment. *Land Degrad. Develop.* 26, 45–53. doi:10.1002/ldr.2293

Li, H., Meng, F., Duan, W., Lin, Y., and Zheng, Y. (2019). Biodegradation of Phenol in saline or Hypersaline Environments by Bacteria: A Review. *Ecotoxicology Environ. Saf.* 184, 109658. doi:10.1016/j.ecoenv.2019.109658

Liang, L., Luo, L., and Zhang, S. (2011). Adsorption and Desorption of Humic and Fulvic Acids on SiO2 Particles at Nano- and Micro-scales. *Colloids Surf. A: Physicochemical Eng. Aspects* 384, 126–130. doi:10.1016/j.colsurfa.2011.03.045

Liu, K., Ding, X., Tang, X., Wang, J., Li, W., Yan, Q., et al. (2018). Macro and Microelements Drive Diversity and Composition of Prokaryotic and Fungal Communities in Hypersaline Sediments and Saline–Alkaline Soils. *Front. Microbiol.* 9, 352. doi:10.3389/fmicb.2018.00352

Lorenz, K., Lal, R., Preston, C. M., and Nierop, K. G. J. (2007). Strengthening the Soil Organic Carbon Pool by Increasing Contributions from Recalcitrant Aliphatic Bio(macro)molecules. *Geoderma* 142, 1–10. doi:10.1016/j.geoderma.2007.07.013

Lu, H., Zhao, C., Joseph, M., Yi, S., Zhao, H., Zhou, Y., et al. (2011). Holocene Climatic Changes Revealed by Aeolian Deposits from the Qinghai Lake Area (Northeastern Qinghai-Tibetan Plateau) and Possible Forcing Mechanisms. *The Holocene* 21, 297–304.

Lü, W. C., Yang, Z. J., Zhou, Y. Z., Li, H. Z., Zeng, X. Q., Chen, Q., et al. (2013). [Spectral Characteristics and Implications of Quartz from Heliao lead-zinc Polymetallic Ore District in the South of Qinzhou-Hangzhou Joint belt]. *Guang Pu Xue Yu Guang Pu Fen Xi* 33, 1374–1378. doi:10.3964/j.issn.1000-0593(2013)05-1374-05

Lücke, A., and Brauer, A. (2004). Biogeochemical and Micro-facial Fingerprints of Ecosystem Response to Rapid Late Glacial Climatic Changes in Varved

Sediments of Meerfelder Maar (Germany). *Palaeogeogr. Palaeoclimatol. Palaeoecol.* 211, 139–155. doi:10.1016/j.palaeo.2004.05.006

Ma, Q., Zhu, L., Lü, X., Wang, J., Ju, J., Kasper, T., et al. (2019). Late Glacial and Holocene Vegetation and Climate Variations at Lake Tangra Yumco, central Tibetan Plateau. *Glob. Planet. Change* 174, 16–25. doi:10.1016/j.gloplacha.2019.01.004

Ma, Z., Han, F., Chen, T., Yi, L., Lu, X., Chen, F., et al. (2021). The Forming Age and the Evolution Process of the Brine Lithium Deposits in the Qaidam Basin Based on Geochronology and Mineral Composition. *Front. Earth Sci.* 9, 702223. doi:10.3389/feart.2021.702223

Means, J. C. (1995). Influence of Salinity upon Sediment-Water Partitioning of Aromatic Hydrocarbons. *Mar. Chem.* 51, 3–16. doi:10.1016/0304-4203(95)00043-q

Meyers, P. A. (2003). Applications of Organic Geochemistry to Paleolimnological Reconstructions: a Summary of Examples from the Laurentian Great Lakes. *Org. Geochem.* 34, 261–289. doi:10.1016/s0146-6380(02)00168-7

Meyers, P. A., and Ishiwatari, R. (1993). Lacustrine Organic Geochemistry-An Overview of Indicators of Organic Matter Sources and Diagenesis in lake Sediments. *Org. Geochem.* 20, 867–900. doi:10.1016/0146-6380(93)90100-p

Meyers, P. A., and Teranes, J. L. (2001). "Sediment Organic Matter," in Tracking Environmental Change Using Lake Sediments: Physical And Geochemical Methods *Developments in Paleoenvironmental Research*. Editors W. M. Last and J. P. Smol (Dordrecht: Springer Netherlands), 239–269. doi:10.1007/0-306-47670-3_9

Muri, G., and Wakeham, S. G. (2006). Organic Matter and Lipids in Sediments of Lake Bled (NW Slovenia): Source and Effect of Anoxic and Oxic Depositional Regimes. *Org. Geochem.* 37, 1664–1679. doi:10.1016/j.orggeochem.2006.07.016

Ndwigah, F. I., Boga, H., Wanyoike, W., and Kachiuri, R. (2013). Enzymatic Activity, and Secondary Metabolites of Fungal Isolates from Lake Sonachi in Kenya. *JKUAT Annu. Sci. Conf. Proc.*, 106–120.

Nichols, P. D., Palmisano, A. C., Rayner, M. S., Smith, G. A., and White, D. C. (1990). Occurrence of Novel C30 Sterols in Antarctic Sea-Ice Diatom Communities during a spring Bloom. *Org. Geochem.* 15, 503–508. doi:10.1016/0146-6380(90)90096-i

Oh, S. Y., Yoo, D. I., Shin, Y., and Seo, G. (2005). FTIR Analysis of Cellulose Treated with Sodium Hydroxide and Carbon Dioxide. *Carbohydr. Res.* 340, 417–428. doi:10.1016/j.carres.2004.11.027

Omar, Z., Bouajila, A., Bouajila, J., Rahmani, R., Besser, H., and Hamed, Y. (2020). Spectroscopic and Chromatographic Investigation of Soil Organic Matter Composition for Different Agrosystems from Arid saline Soils from Southeastern Tunisia. *Arab. J. Geosci.* 13, 524. doi:10.1007/s12517-020-05569-3

Parolo, M. E., Savini, M. C., and Loewy, R. M. (2017). Characterization of Soil Organic Matter by FT-IR Spectroscopy and its Relationship with Chlorpyrifos Sorption. *J. Environ. Manage.* 196, 316–322. doi:10.1016/j.jenvman.2017.03.018

Pearson, A., and Eglinton, T. I. (2000). The Origin of N -alkanes in Santa Monica Basin Surface Sediment: a Model Based on Compound-specific Δ 14 C and δ 13 C Data. *Org. Geochem.* 31, 1103–1116. doi:10.1016/s0146-6380(00)00121-2

Peyton, B. M., Wilson, T., and Yonge, D. R. (2002). Kinetics of Phenol Biodegradation in High Salt Solutions. *Water Res.* 36, 4811–4820. doi:10.1016/s0043-1354(02)00200-2

Piechulla, B., and Degenhardt, J. (2014). The Emerging Importance of Microbial Volatile Organic Compounds. *Plant Cel Environ* 37, 811–812. doi:10.1111/pce.12254

Pongpiachan, S., Thumanu, K., Phatthalung, W., Tipmanee, D., Kanchai, P., Feldens, P., et al. (2013). Using Fourier Transform Infrared (FTIR) to Characterize Tsunami Deposits in Near-Shore and Coastal Waters of Thailand. *J. Tsunami Soc. Int.* 32, 39–57.

Prokopenko, A. A., Williams, D. F., Karabanov, E. B., and Khursevich, G. K. (1999). Response of Lake Baikal Ecosystem to Climate Forcing and pCO2 Change over the Last Glacial/interglacial Transition. *Earth Planet. Sci. Lett.* 172, 239–253. doi:10.1016/s0012-821x(99)00203-4

Quicksall, A. N., Bostick, B. C., and Sampson, M. L. (2008). Linking Organic Matter Deposition and Iron mineral Transformations to Groundwater Arsenic Levels in the Mekong delta, Cambodia. *Appl. Geochem.* 23, 3088–3098. doi:10.1016/j.apgeochem.2008.06.027

Rahier, H., Wullaert, B., and Van Mele, B. (2000). Influence of the Degree of Dehydroxylation of Kaolinite on the Properties of Aluminosilicate Glasses. *J. Therm. Anal. Calorim.* 62, 417–427. doi:10.1023/a:1010138130395

Ramasamy, V., Rajkumar, P., and Ponnusamy, V. (2009). Depth wise Analysis of Recently Excavated Vellar River Sediments through FTIR and XRD Studies. *Indian J. Phys.* 83, 1295–1308. doi:10.1007/s12648-009-0110-3

Riedel, T., Zak, D., Biester, H., and Dittmar, T. (2013). Iron Traps Terrestrially Derived Dissolved Organic Matter at Redox Interfaces. *Proc. Natl. Acad. Sci.* 110, 10101–10105. doi:10.1073/pnas.1221487110

Robinson, N., Cranwell, P. A., Eglinton, G., Brassell, S. C., Sharp, C. L., Gophen, M., et al. (1986). Lipid Geochemistry of Lake Kinneret. *Org. Geochem.* 10, 733–742. doi:10.1016/s0146-6380(86)80010-9

Rosa, E., Dębska, B., Banach-Szott, M., and Tobiasova, E. (2016). Use of Hplc, Py-Gcms, Ftir Methods in the Studies of the Composition of Soil Dissolved Organic Matter. *pjss* 48, 101. doi:10.17951/pjss.2015.48.1.101

Sachse, D., Radke, J., and Gleixner, G. (2004). Hydrogen Isotope Ratios of Recent Lacustrine Sedimentary N-Alkanes Record Modern Climate Variability. *Geochimica et Cosmochimica Acta* 68, 4877–4889. doi:10.1016/j.gca.2004.06.004

Sarkhot, D. V., Comerford, N. B., Jokela, E. J., Reeves, J. B., and Harris, W. G. (2007). Aggregation and Aggregate Carbon in a Forested Southeastern Coastal Plain Spodosol. *Soil Sci. Soc. Am. J.* 71, 1779–1787. doi:10.2136/sssaj2006.0340

Schie, P. M. van., and Young, L. Y. (2000). Biodegradation of Phenol: Mechanisms and Applications. *Bioremediation J.* 4, 1–18.

Schmidt, R., Cordovez, V., de Boer, W., Raaijmakers, J., and Garbeva, P. (2015). Volatile Affairs in Microbial Interactions. *ISME J.* 9, 2329–2335. doi:10.1038/ismej.2015.42

Senesi, N., D'Orazio, V., and Ricca, G. (2003). Humic Acids in the First Generation of EUROSOILS. *Geoderma* 116, 325–344. doi:10.1016/s0016-7061(03)00107-1

Shanina, S. N. (2002). "Biomarkers in Organic Matter of the Ancient Salt Deposits," in Instruments, Methods, and Missions For Astrobiology Vi *Proceedings of the Society of Photo-Optical Instrumentation Engineers (Spie)*. Editors R. B. Hoover, A. Y. Rozanov, and J. H. Lipps.153–159, Available at: WOS:000181863300020.

Shen, J., Xue, B., Wu, J., Wu, Y., Liu, X., Yang, X., et al. (2010). *Lacustrine Sedimentation and Environmental Evolution*. 2010th ed.. Beijing: Science Press.

Shen, X., Gao, Y., Ding, C., and Archambault, R. (2005). Proceedings Of the 19th Annual International Conference on Supercomputing *ICS '05*. New York, NY, USA: Association for Computing Machinery), 131–140.Lightweight Reference Affinity Analysis.

So, R. T., Blair, N. E., and Masterson, A. L. (2020). Carbonate mineral Identification and Quantification in Sediment Matrices Using Diffuse Reflectance Infrared Fourier Transform Spectroscopy. *Environ. Chem. Lett.* 18, 1725–1730. doi:10.1007/s10311-020-01027-4

Somani, P. R., Marimuthu, R., Viswanath, A. K., and Radhakrishnan, S. (2003). Thermal Degradation Properties of Solid Polymer Electrolyte (Poly(vinyl Alcohol)+phosphoric Acid)/methylene Blue Composites. *Polym. Degrad. Stab.* 79, 77–83. doi:10.1016/s0141-3910(02)00240-9

Stashenko, E., and Martínez, J. R. (2014). Gas Chromatography-Mass Spectrometry. *Adv. Gas Chromatogr.*, 1–38.

Stauch, G. (2015). Geomorphological and Palaeoclimate Dynamics Recorded by the Formation of Aeolian Archives on the Tibetan Plateau. *Earth-Science Rev.* 150, 393–408. doi:10.1016/j.earscirev.2015.08.009

Stauch, G., Schulte, P., Ramisch, A., Hartmann, K., Hülle, D., Lockot, G., et al. (2017). Landscape and Climate on the Northern Tibetan Plateau during the Late Quaternary. *Geomorphology* 286, 78–92. doi:10.1016/j.geomorph.2017.03.008

Strehse, R., Bohne, H., Amha, Y., and Leinweber, P. (2018). The Influence of Salt on Dissolved Organic Matter from Peat Soils. *Org. Geochem.* 125, 270–276. doi:10.1016/j.orggeochem.2018.10.001

Sun, J., Li, S.-H., Muhs, D. R., and Li, B. (2007). Loess Sedimentation in Tibet: Provenance, Processes, and Link with Quaternary Glaciations. *Quat. Sci. Rev.* 26, 2265–2280. doi:10.1016/j.quascirev.2007.05.003

Sun, W., Zhao, S., Pei, H., and Yang, H. (2019). The Coupled Evolution of Mid- to Late Holocene Temperature and Moisture in the Southeast Qaidam Basin. *Chem. Geology.* 528, 119282. doi:10.1016/j.chemgeo.2019.119282

Szymański, W. (2017). Chemistry and Spectroscopic Properties of Surface Horizons of Arctic Soils under Different Types of Tundra Vegetation – A Case Study from the Fuglebergsletta Coastal plain (SW Spitsbergen). *CATENA* 156, 325–337. doi:10.1016/j.catena.2017.04.024

Tfaily, M. M., Chu, R. K., Toyoda, J., Tolić, N., Robinson, E. W., Paša-Tolić, L., et al. (2017). Sequential Extraction Protocol for Organic Matter from Soils and

Sediments Using High Resolution Mass Spectrometry. *Analytica Chim. Acta* 972, 54–61. doi:10.1016/j.aca.2017.03.031

Thompson, L. G., Yao, T., Davis, M. E., Henderson, K. A., Mosley-Thompson, E., Lin, P.-N., et al. (1997). Tropical Climate Instability: The Last Glacial Cycle from a Qinghai-Tibetan Ice Core. *Science* 276, 1821–1825. doi:10.1126/science.276.5320.1821

Tremblay, L., Kohl, S. D., Rice, J. A., and Gagné, J.-P. (2005). Effects of Temperature, Salinity, and Dissolved Humic Substances on the Sorption of Polycyclic Aromatic Hydrocarbons to Estuarine Particles. *Mar. Chem.* 96, 21–34. doi:10.1016/j.marchem.2004.10.004

Tuo, J., Wu, C., Zhang, M., and Chen, R. (2011). Distribution and Carbon Isotope Composition of Lipid Biomarkers in Lake Erhai and Lake Gahai Sediments on the Tibetan Plateau. *J. Great Lakes Res.* 37, 447–455. doi:10.1016/j.jglr.2011.05.018

Valdrè, G., Moro, D., and Ulian, G. (2012). Mineral Surface–Organic Matter Interactions: Basics and Applications. *IOP Conf. Ser. Mater. Sci. Eng.* 32, 012027. doi:10.1088/1757-899x/32/1/012027

Vane, C. H., Kim, A. W., Moss-Hayes, V., Snape, C. E., Diaz, M. C., Khan, N. S., et al. (2013). Degradation of Mangrove Tissues by Arboreal Termites (Nasutitermes Acajutlae) and Their Role in the Mangrove C Cycle (Puerto Rico): Chemical Characterization and Organic Matter Provenance Using Bulk δ 13 C, C/N, Alkaline CuO oxidation-GC/MS, and Solid-state 13 C NMR. *Geochem. Geophys. Geosyst.* 14, 3176–3191. doi:10.1002/ggge.20194

Volkman, J. K., Farrington, J. W., and Gagosian, R. B. (1987). Marine and Terrigenous Lipids in Coastal Sediments from the Peru Upwelling Region at 15°S: Sterols and Triterpene Alcohols. *Org. Geochem.* 11, 463–477. doi:10.1016/0146-6380(87)90003-9

Wang, X.-C., and Lee, C. (1993). Adsorption and Desorption of Aliphatic Amines, Amino Acids and Acetate by clay Minerals and marine Sediments. *Mar. Chem.* 44, 1–23. doi:10.1016/0304-4203(93)90002-6

Wang, Y., Fang, X., Bai, Y., Xi, X., Zhang, X., and Wang, Y. (2007). Distribution of Lipids in Modern Soils from Various Regions with Continuous Climate (Moisture-heat) Change in China and Their Climate Significance. *Sci. China Ser. D* 50, 600–612. doi:10.1007/s11430-007-2062-9

Wilson, H. F., and Xenopoulos, M. A. (2009). Effects of Agricultural Land Use on the Composition of Fluvial Dissolved Organic Matter. *Nat. Geosci* 2, 37–41. doi:10.1038/ngeo391

Wirrmann, D., Bertaux, J., and Kossoni, A. (2001). Late Holocene Paleoclimatic Changes in Western Central Africa Inferred from Mineral Abundance in Dated Sediments from Lake Ossa (Southwest Cameroon). *Quat. Res.* 56, 275–287. doi:10.1006/qres.2001.2240

Wischnewski, J., Mischke, S., Wang, Y., and Herzschuh, U. (2011). Reconstructing Climate Variability on the Northeastern Tibetan Plateau since the Last Lateglacial - a Multi-Proxy, Dual-Site Approach Comparing Terrestrial and Aquatic Signals. *Quat. Sci. Rev.* 30, 82–97. doi:10.1016/j.quascirev.2010.10.001

Wu, T., Li, J., and Yang, M. (2018). The Aeolian Bedforms and the Reconstruction of Late Holocene Wind Direction in Qaidam Basin. *Acta Sci. Nat. Univ. Pekin.* 54, 1021–1027.

Wu, X., Wang, Z., and He, Z. (2012). Implications of TS /TOC for Sedimentary Environments of the Southern Changjiang delta plain. *J. Palaeogeogr.* 14, 821–828.

Wu, Y., Zhang, J., and Yu, Z. (2001). Distribution of Lipids in the Core Sediments of the Bohai. *Acta Scicentiarum Nat. Univ. Pekinesis* 37, 273–277. doi:10.13209/j.0479-8023.2001.055

Xiang, S., Zeng, F., Wang, G., and Yu, J. (2013). Environmental Evolution of the South Margin of Qaidam Basin Reconstructed from the Holocene Loess deposit by N-Alkane and Pollen Records. *J. Earth Sci.* 24, 170–178. doi:10.1007/s12583-013-0320-7

Yang, D. S., Shewfelt, R. L., Lee, K.-S., and Kays, S. J. (2008). Comparison of Odor-Active Compounds from Six Distinctly Different Rice Flavor Types. *J. Agric. Food Chem.* 56, 2780–2787. doi:10.1021/jf072685t

Yang, X. (2015). *Modern Flood Process and the OSL Dating and Grain-Size Characteristic on Palaeoflood Deposits of Nalinggele Watershed, Northern of the Qinghai-Tibet Plateau*. Master thesis. (Xining: Qinghai Normal University).

Yu, L., and Lai, Z. (2012). OSL Chronology and Palaeoclimatic Implications of Aeolian Sediments in the Eastern Qaidam Basin of the Northeastern Qinghai-Tibetan Plateau. *Palaeogeogr. Palaeoclimatol. Palaeoecol.* 337-338, 120–129. doi:10.1016/j.palaeo.2012.04.004

Yu, Y., Lin, K., Zhou, X., Wang, H., Liu, S., and Ma, X. (2007). New C−H Stretching Vibrational Spectral Features in the Raman Spectra of Gaseous and Liquid Ethanol†. *J. Phys. Chem. C* 111, 8971–8978. doi:10.1021/jp0675781

Zeng, F., Xiang, S., Zhang, K., and Lu, Y. (2011). Environmental Evolution Recorded by Lipid Biomarkers from the Tawan Loess-Paleosol Sequences on the West Chinese Loess Plateau during the Late Pleistocene. *Environ. Earth Sci.* 64, 1951–1963. doi:10.1007/s12665-011-1012-1

Zhang, P., Yu, S., Zhi, X., Zheng, X., Li, J., Li, B., et al. (1987). *Salt Lake in Qaidam Basin*. Beijing: Science Press.

Zhao, J., Jin, Z., Jin, Z., Hu, Q., Hu, Z., Du, W., et al. (2017a). Mineral Types and Organic Matters of the Ordovician-Silurian Wufeng and Longmaxi Shale in the Sichuan Basin, China: Implications for Pore Systems, Diagenetic Pathways, and Reservoir Quality in fine-grained Sedimentary Rocks. *Mar. Pet. Geology.* 86, 655–674. doi:10.1016/j.marpetgeo.2017.06.031

Zhao, J., Jin, Z., Jin, Z., Wen, X., and Geng, Y. (2017b). Origin of Authigenic Quartz in Organic-Rich Shales of the Wufeng and Longmaxi Formations in the Sichuan Basin, South China: Implications for Pore Evolution. *J. Nat. Gas Sci. Eng.* 38, 21–38. doi:10.1016/j.jngse.2016.11.037

Zhao, M., Dupont, L., Eglinton, G., and Teece, M. (2003). n-Alkane and Pollen Reconstruction of Terrestrial Climate and Vegetation for N.W. Africa over the Last 160 Kyr. *Org. Geochem.* 34, 131–143. doi:10.1016/s0146-6380(02)00142-0

Zhao, Y., Song, K., Wen, Z., Li, L., Zang, S., Shao, T., et al. (2016). Seasonal Characterization of CDOM for Lakes in Semiarid Regions of Northeast China Using Excitation-Emission Matrix Fluorescence and Parallel Factor Analysis (EEM-PARAFAC). *Biogeosciences* 13, 1635–1645. doi:10.5194/bg-13-1635-2016

Zheng, M., and Liu, X. (2009). Hydrochemistry of Salt Lakes of the Qinghai-Tibet Plateau, China. *Aquat. Geochem.* 15, 293–320. doi:10.1007/s10498-008-9055-y

Zheng, M. (2011). Resources and Eco-Environmental protection of Salt Lakes in China. *Environ. Earth Sci.* 64, 1537–1546. doi:10.1007/s12665-010-0601-8

Zheng, M., Zhang, Y., Liu, X., Qi, W., Kong, F., Nie, Z., et al. (2016). Progress and Prospects of Salt Lake Research in China. *Acta Geol. Sin. - Engl. Ed.* 90, 1195–1235. doi:10.1111/1755-6724.12767

Zhu, G., Jin, Q., Zhang, S. W., Zhang, L. Y., and Chun, G. (2004). Salt lake-saline lake Sedimentary Combination and Petroleum Accumulation in the Bonan Sag. *Acta Mineral. Sin.* 1, 25–30. doi:10.16461/j.cnki.1000-4734.2004.01.005

Zhuang, K., Wu, N., Wang, X., Wu, X., Wang, S., Long, X., et al. (2016). Effects of 3 Feeding Modes on the Volatile and Nonvolatile Compounds in the Edible Tissues of Female Chinese Mitten Crab (Eriocheir Sinensis). *J. Food Sci.* 81, S968–S981. doi:10.1111/1750-3841.13229

Conflict of Interest: The authors declare that the research was conducted in the absence of any commercial or financial relationships that could be construed as a potential conflict of interest.

Publisher's Note: All claims expressed in this article are solely those of the authors and do not necessarily represent those of their affiliated organizations, or those of the publisher, the editors and the reviewers. Any product that may be evaluated in this article, or claim that may be made by its manufacturer, is not guaranteed or endorsed by the publisher.